Available online at www.sciencedirect.com
SCIENCE DIRECT®

Journal of the European Ceramic Society 24 (2004) 17–23

www.elsevier.com/locate/jeurceramsoc

The role of Si–O species in the colloidal stability of silicon-containing ceramic powders

Yoko Fukada, Patrick S. Nicholson*

Department of Materials Science and Engineering, McMaster University, 1280 Main Street West, Hamilton, Ontario, Canada L8S 4L7

Received 18 October 2002; received in revised form 27 February 2003; accepted 7 March 2003

Abstract

The relative colloidal stability in ethanol of ceramic powders with Si–O surface groups (Si_3N_4, SiC and $MoSi_2$) is reported. SiO_2/EtOH suspensions are also examined as reference. The comparative relationships between pH, particle-surface charge, zeta-potential, stability and suspension rheology are discussed. The nature and influence of the surface species is determined and the similarity/difference therebetween, compared. DLVO theory and Stability Ratio values defined suspension stability and it was found non-oxide particles in EtOH are charged-stabilized and have viscosity and flow-curves that agree with the electrokinetic measurements.

Keywords: Colloidal stability; $MoSi_2$; SiC; Si_3N_4; SiO_2; Suspensions

1. Introduction

It is common wisdom that Si-containing ceramic powders form Si–O surface layers. This paper explores and extends this assumption by defining the species present on Si_3N_4, SiC and $MoSi_2$ and their influence on ethanol suspension stability.

Ethanol is employed as it contains sufficient H_2O (0.2 wt.%) to confer ionic stability but too little to produce deleterious electrolysis gases during processing by electrophoretic deposition (EPD).[1] EPD can be performed in aqueous suspensions but dense films are difficult to obtain because of water electrolysis. Nonaqueous EPD has thus been explored.[2–4]

The stability of particles in suspension is due to surface charge and the resulting ionic atmosphere entropic effects (“ionic” stabilization), or the presence of adsorbed layers that physically limit inter-particle approach (steric stabilization). Ionic stabilization is effective in high-dielectric-constant media, e.g. water. However, it also plays a role in nonaqueous solvents[5,6] especially those with minor water content.

Silicon nitride (Si_3N_4), silicon carbide (SiC) and molybdenum disilicide ($MoSi_2$) are important, high performance ceramic materials which are thought protected from further oxidation by surface layers of “SiO_2” (the amorphous SiO_2-based oxides). Thus the colloidal stability of Si_3N_4, SiC and $MoSi_2$ in EtOH is compared with amorphous silica (SiO_2) in EtOH, as reference.

2. Experimental

High purity, α-silicon nitride powder (H.C. Starck M11, Berlin, Germany) (average particle size: 0.63 μm, Oxygen: 1.32%, 93.3% α-phase), silicon carbide (SiC) powder (Ibiden, Ultrafine, Japan) (average particle size: 0.29 μm, β-phase) and molybdenum disilicide ($MoSi_2$) powder (Cerac, M-1103, USA) (average particle size: 1.74 μm, crystalline) were investigated. The specific surface area of the Si_3N_4, SiC and $MoSi_2$ were determined as 11.20, 21.99 and 0.32 m^2/g, respectively by the BET method (Autosorb Automated Gas Adsorption System). Anhydrous, absolute ethyl alcohol (EtOH) (Alcohol Inc.) (0.2 wt.% water) was used as solvent.

XPS (Leybold Max 200) was used to analyze the chemical composition of surface films. The spectrometer is equipped with a Mg K_α, unmonochromatic, X-ray

* Corresponding author. Tel.: +1-905-525-9140; fax: +1-905-528-9295.
E-mail address: nicholsn@mcmaster.ca (P.S. Nicholson).

0955-2219/03/$ - see front matter © 2003 Published by Elsevier Ltd.
doi:10.1016/S0955-2219(03)00124-9

source. Spectra were satellite-subtracted and normalised to correct for unit transmission. The spectral regions of particular interest were run in high-resolution mode (Pass Energy = 48 eV).

The electrophoretic mobility and specific conductivity of 0.01 wt.% suspensions were measured by Coulter DELSA (Doppler Electrophoretic Light Scattering Analyzer) 440 (Coulter Electronics, FL, USA) at various pH values and 25.0±0.3 °C. Suspension pH was adjusted with glacial acetic acid (HAc), hydrochloric acid (HCl) or tetramethyl ammonium hydroxide (TMAH). All suspensions were ultrasonicated for 5 min. before measurement. Zeta potentials were calculated via the O'Brien and White[7] computer program or via Henry's equation.

pH was measured with a pH meter (Accumet 1002, Fisher Scientific Co., PA, USA) at room temperature. The pH meter has glass and calomel electrode pairs with a concentrated aqueous KCl salt bridge. Two aqueous standards of pH 4 and 7 were used for standardization due to the lack of standard buffer solutions for EtOH. The pH meter determines so-called "operational pH values" for non-aqueous solvents. The pH value used in this paper is the "operational pH". The theoretical background and method involving operational pH was described by Wang et al.[8] They explained in any medium, the operational pH differs from the actual pH (pa_H) by the residual liquid-junction potential, ΔE_j:

$$pH - pa_H = \frac{\Delta E_j}{0.05916} \quad \text{at } 25\ ^\circ C \tag{1}$$

where pH is the pH meter reading, and a_H the hydrogen-ion activity. The ΔE_j value between an aqueous KCl bridge and dilute nonaqueous solutions is primarily a function of the solvent, and the quantity $(\Delta E_j/0.05916) - \log {}_m\gamma_H$ ($= \delta$) is approximately constant for a given solvent medium, independent of the activity of the solution (${}_m\gamma_H$ is the transfer activity coefficient). Eq. (1) can be rewritten as

$$pa_H = pH - \delta - \log {}_{m\gamma H} = pH - \frac{\Delta E_j}{0.05916} \quad \text{at } 25^\circ C. \tag{2}$$

when δ and $\log {}_m\gamma_H$ are known for a given solvent, the pa_H of its solutions can be evaluated directly from operational pH readings conducted in a nonaqueous medium.[8,9]

Rheological measurements were conducted at 25 °C in a Bohlin, controlled-shear-rate VOR rheometer (Bohlin Rheologie, Lund, Sweden). A concentric cylinder measuring system was used with a moving cup 27.5 mm radius and a fixed bob 25.0 mm radius. A range of shear rates was applied to the samples. This range was programmed to sweep from the lowest value to the highest value, in steps (each step at a fixed shear rate); then the order reversed. The viscosity and shear-stress were measured over a 20 s period. The 15 vol.% solids suspensions were prepared using a Sonicator (Ultrasonic Processor XL, MISONIX) for 10 min to achieve well-dispersed, homogeneous dispersion.

3. Results and discussion

3.1. The surface chemistry of Si_3N_4, SiC and $MoSi_2$ powders in EtOH

Table 1 shows the atomic percent oxygen on the surface of the as-received Si_3N_4, SiC, $MoSi_2$ powders and SiO_2 powder as reference. All powders exhibit the O(1s) peak, i.e. there are oxide layers on all the powders. The atomic% O(1s) on $MoSi_2$ and SiO_2 are 57.26 and 62.36%, respectively, i.e. most of the surface is silica, the probable group being silanol, i.e. acidic. The atomic% O(1s) on Si_3N_4 (13.14%) and SiC (13.71%) is similar and lower than on $MoSi_2$ and SiO_2, i.e., the surfaces are only partially covered by oxide. Except for the SiC, the C(1s) values observed are thought associated with impurities. $MoSi_2$ has high carbon impurity. The Si(2p) level on $MoSi_2$ is lower than the other powders. The value of Mo(3d) is also low. These results suggest $MoSi_2$ powder is completely covered by an "oxide" that is not exclusively "SiO_2".

Fig. 1 shows the electrophoretic mobility versus pH for Si_3N_4, SiC, $MoSi_2$ and SiO_2[6] powders in EtOH. All suspension electrophoretic mobilities are pH-dependent. The surfaces are positively charged for $pH < pH_{iep}$ (the isoelectric point) and negatively charged for $pH > pH_{iep}$. The pH_{iep} is 9.0 for Si_3N_4, 5.4 for SiC, 2.2 for $MoSi_2$ and 1.4 for SiO_2. All powder surfaces display silanol (Si–OH) groups. When this film thickens, the pH_{iep} approaches the value for silica (pH = 1.4). This is demonstrated in Fig. 2, the electrophoretic mobility versus pH for oxidized Si_3N_4 (1200 °C, 1 h in air) in EtOH. The pH_{iep} shifts towards the value for silica.

The difference of pH_{iep} between Si_3N_4 and SiC can be explained by the dissociation reactions of their surface groups. The main surface group for both powders is Si–OH and the possible dissociation reactions are:

$$Si-OH_2^+ \longleftrightarrow Si-OH + H^+ \tag{3}$$

$$Si-OH \longleftrightarrow Si-O^- + H^+ \tag{4}$$

Table 1
XPS results: atomic% for as-received Si_3N_4, SiC, $MoSi_2$ and SiO_2

	Si_3N_4	SiC	$MoSi_2$	SiO_2
O (1s)	13.14	13.71	57.26	62.36
N (1s)	42.22	–	–	–
C (1s)	6.21	55.33	15.46	5.13
Mo (3d)	–	–	6.30	–
Si (2p)	38.43	30.97	20.98	32.52

An additional basic amine group can exist on Si_3N_4. The dissociation reaction thereof is:[10]

$$Si_2NH_2^+ \longleftrightarrow Si_2{-}NH + H^+ \quad (5)$$

The ratio acidic/basic groups determines the charge behaviour of Si_3N_4 powder in EtOH and hence the pH_{iep}. A high concentration of silanol shifts the pH_{iep} to lower pH values whereas amine groups shift it to higher values.[10]

Oxycarbide, SiO_2C_2 and SiO_3C species have been found on SiC[11] so the concentration of silanol on SiC is expected less than silica (Table 1), i.e. the pH_{iep} will be higher than for SiO_2.

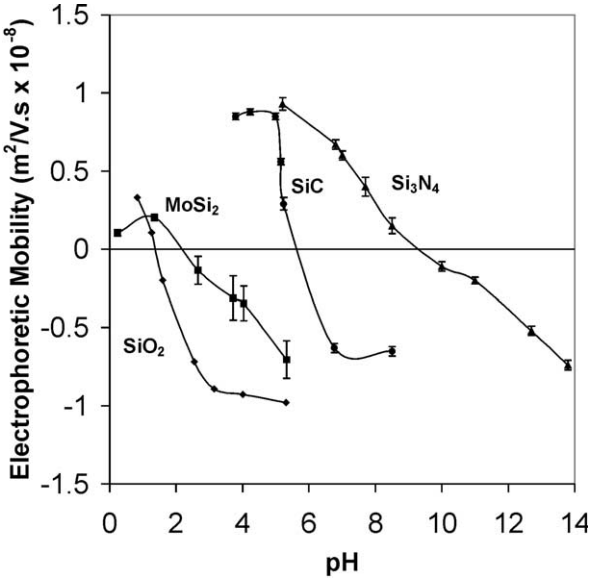

Fig. 1. Electrophoretic mobility versus pH for Si_3N_4, SiC, $MoSi_2$ and SiO_2 in EtOH, SiO_2 data from Wang.[6] (The error bars are 90% confidence intervals by using Komagata curve.)

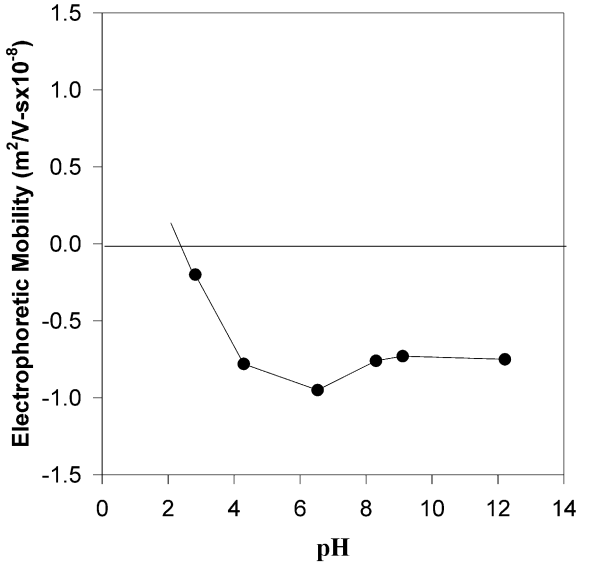

Fig. 2. Electrophoretic mobility versus pH for the oxidized Si_3N_4 in EtOH.

$MoSi_2$ powder, on the other hand, is completely covered by oxide yet its pH_{iep} is higher than that of SiO_2. This means Mo-oxide species must co-exist on the surface (Table 1). The pH_{iep} for $MoSi_2$ is higher than SiO_2 as the silanol group concentration on the former is less than on the latter.

3.2. The stability in the Si_3N_4-, SiC-, $MoSi_2$- EtOH systems

3.2.1. Via DLVO theory

The stability of Si_3N_4, SiC and $MoSi_2$ particles in EtOH depends on the total potential interaction energy between particles, V_T, i.e. $V_T = V_R + V_A$ where V_R is the repulsion potential energy and V_A the attractive one. Fig. 3 shows the total potential energy (V_T) as a function of particle separation distance (H) for Si_3N_4/EtOH. The necessary potential energies, V_R and V_A, were calculated via,[12]

$$V_R(sp) = 2\pi\varepsilon_o\varepsilon_r a\psi_o^2 \ln[1 + \exp(-\kappa H)] \quad (6)$$

where ε_r is the relative dielectric constant of the medium, ε_o the dielectric constant of vacuum, a the particle radius, ψ_o the surface potential, κ the Debye-Hückel parameter and H the shortest distance between two particles. $\psi_O = \zeta$ is assumed (known to be valid for organic media) and the zeta-potential, ζ is calculated from experimentally-obtained electrophoretic mobility data. V_A is calculated via:[12]

$$V_A = -\frac{A}{6}\left[\frac{2}{s^2-4} + \frac{2}{s^2} + \ln\left(\frac{s^2-4}{s^2}\right)\right] \quad (7)$$

where $s = \frac{H}{a} + 2$. The Hamaker Constant A is replaced by $A_{11(3)}$ (where two particles of material 1 suspended in

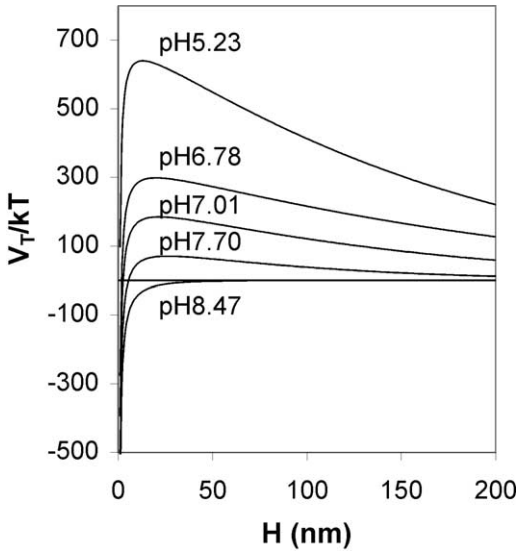

Fig. 3. Calculated interaction energies between two positively charged Si_3N_4 particles in EtOH.

medium 3), for α-Si_3N_4 in EtOH (9.5 kT), for β-SiC in EtOH (28 kT) and for $MoSi_2$ in EtOH (8.0 kT). (These values were calculated from Refs. 13–16.)

The positive zeta-potential curves for Si_3N_4 /EtOH (Fig. 3) at pH = 5.23, 6.78 and 7.01 have energy barriers > 100 kT thus the particles are ionically stable. pH = 7.70 and 8.47 have no energy barrier so the suspensions are unstable. pH = 13.8 and 12.7 (the same way to draw the DLVO curves as Fig. 3) have energy barriers > 80 kT, indicating stability but pH = 11.0 and 9.10 have a zero energy barrier (pH_{iep} = 9.0) so the suspensions are considered unstable. Acidic Si_3N_4/EtOH suspensions are more stable than basic ones.

Suspensions of SiC/EtOH with pH = 4.23, 4.99, 3.79 and 5.15 have energy barriers > 70 kT. The (pH = 3.79) suspension is less stable because the necessary high-HAc-concentration compresses the double-layer, reducing the zeta-potential. A small change of pH renders SiC/EtOH unstable as the electrophoretic mobility changes sharply with pH (Fig. 1). Suspensions with pH = 6.76 and 8.50 are stable but pH = 13.8 is unstable because of double-layer compression. SiC/EtOH suspensions also became unstable as the pH value approaches the pH_{iep}. Again acidic suspensions are more stable.

$MoSi_2$/EtOH has a negative zeta-potential at pH = 5.33 with an energy barrier > 70 kT, indicating stability. The suspensions for pH < 5 suggest instability. Thus $MoSi_2$/EtOH differs from Si_3N_4/EtOH and SiC/EtOH and its pH_{iep} is lower, i.e. pH = 2.2, closer to that of silica. Negatively-charged lyosphere systems are more stable than positively charged ones for $MoSi_2$/EtOH as the pH region for positively charged $MoSi_2$ is pH < 2. The concentration of acid thereat is so high, compression of the double layer occurs with resultant suspension instablility. Also the larger particle size of the $MoSi_2$ powder and its higher density tend to induce settling vis à vis Si_3N_4 and SiC.

3.3. Via stability-ratio and suspension stability

The stability ratio (W) is the ratio of the most rapid coagulation rate for a suspension (J_r) to an actual, slower rate (J_s), i.e. $W = J_r/J_s$. W increases with increasing interparticle repulsive energy, i.e. higher values of W mean higher suspension stability. In the present work, stability ratios were calculated via (MathCad computer software);

$$W = 2\int_0^{\infty} \exp\left(\frac{V_T}{kT}\right)\frac{ds}{s^2} \tag{8}$$

Plots of log W versus pH for Si_3N_4/, SiC/, and $MoSi_2$/EtOH are shown in Fig. 4. (log W < 10 indicates instability, i.e. in the region of pH_{iep}). Stability increases for pH < pH_{iep} and pH > pH_{iep}.

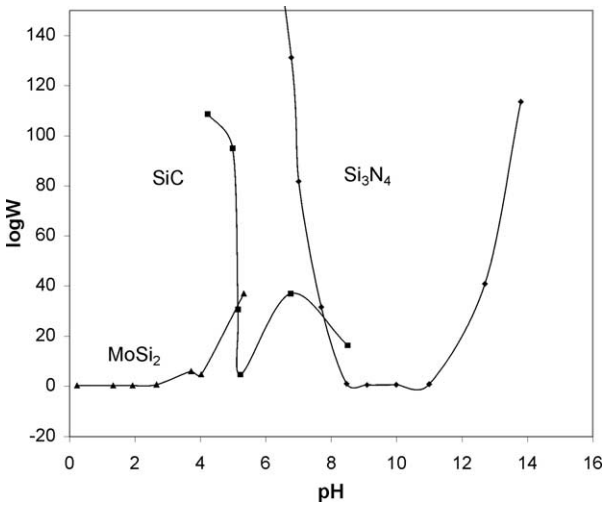

Fig. 4. log W versus pH for Si_3N_4/, SiC/, and $MoSi_2$/EtOH.

3.4. Via the rheology of Si_3N_4/EtOH, SiC/EtOH and $MoSi_2$/EtOH suspensions

Figs. 5 and 6 show viscosity vs. shear-rate for 0.15vol% for Si_3N_4/EtOH and SiC/EtOH at different pH values. All suspensions exhibit shear-thinning. The flow curves were fitted to the Casson equation:[17]

$$S^{1/2} = S_c^{1/2} + (u_c \cdot D)^{1/2} \tag{9}$$

where S is the shear stress (Pa), S_c, the Casson yield stress (Pa), D, the shear rate (1/s) and u_c, the Casson viscosity (Pas). The best fit (solid lines in Figs. 7 and 8) to the data was plotted.

According to the Casson model, particles in a flocculated suspension form flocs (networks) because of mutual attraction. The Casson yield value, S_c, is a measure of the degree of flocculation and is pH-dependent (Figs. 9 and 10). The maximum S_c corresponds to

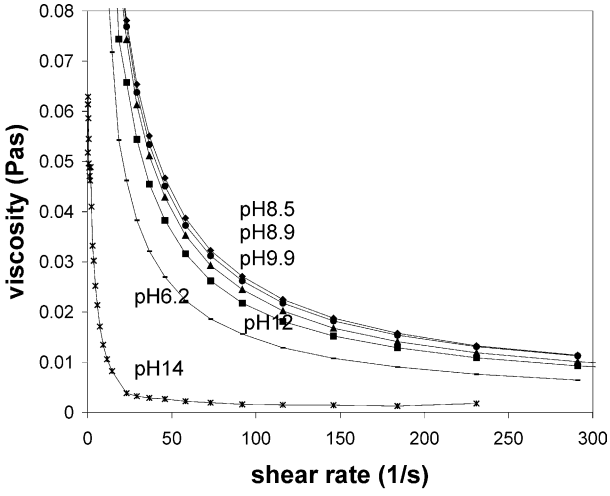

Fig. 5. The viscosity versus the shear-rate for EtOH suspensions containing 0.15 volume-fraction of Si_3N_4 powder at different pH values.

pH_{iep} ($Si_3N_4 = 8.9$; $SiC = 5.4$) in agreement with the electrokinetic results i.e. Si_3N_4; 9.0 and SiC; 5.4.

Fig. 10 (SiC/EtOH) shows S_c decreases to a minimum with pH; then it increases. The latter is due to acid compression of the double layer and concomitant instability.

The yield stress of SiC/EtOH is less than the value for Si_3N_4/EtOH for most pH values. This result is possibly due to the carbon of SiC having a higher affinity for EtOH molecules so SiC particles flow more easily than Si_3N_4 particles.

The $MoSi_2$/EtOH system exhibits different viscosity vs. shear rate behaviour (Fig. 11). Viscosity increases with shear rate, i.e. the suspension is dilatent. This suggests EtOH does not 'wet' the $MoSi_2$ as strongly as Si_3N_4 and SiC resulting in particle flocculation and shear-thickening. The $MoSi_2$/EtOH system does not follow the Casson model because of this dilatancy. The highest viscosity occurs at pH = 2.2 at a shear-rate of, 231 s^{-1}. This is the pH_{iep} value via electrokinetic measurement.

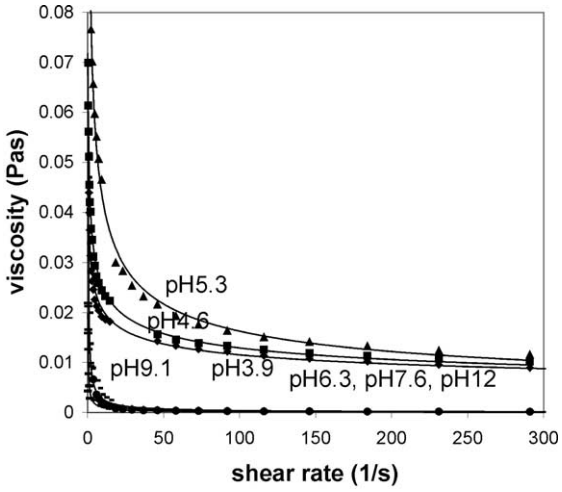

Fig. 6. The viscosity versus the shear-rate for EtOH suspensions containing 0.15 volume-fraction of SiC powder at different pH values.

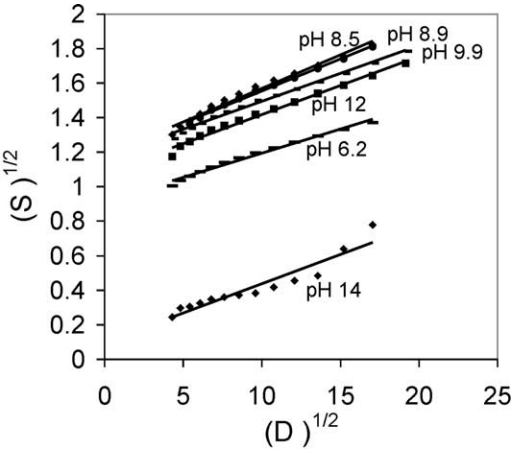

Fig. 7. Casson plot for Si_3N_4 in EtOH at different pH values.

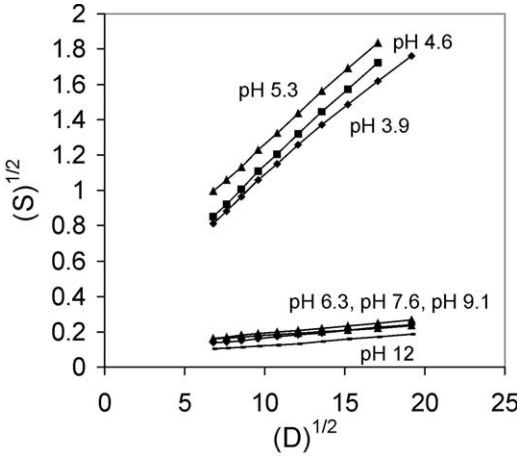

Fig. 8. Casson plot for SiC in EtOH at different pH values.

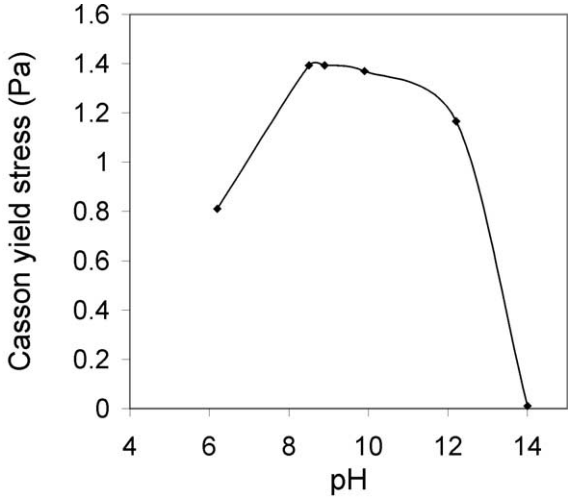

Fig. 9. Casson yield stress versus pH for Si_3N_4 in EtOH.

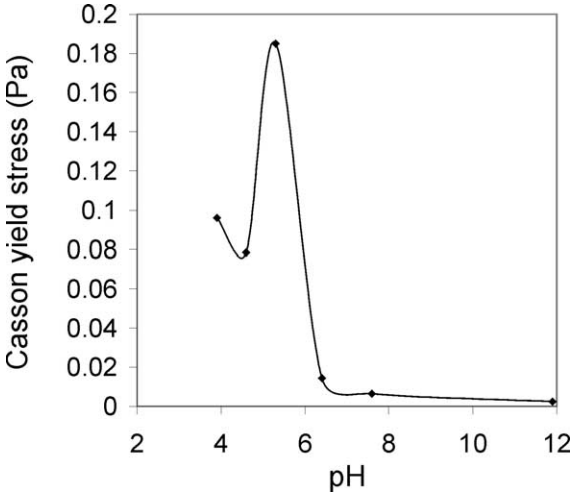

Fig. 10. Casson yield stress versus pH for SiC in EtOH.

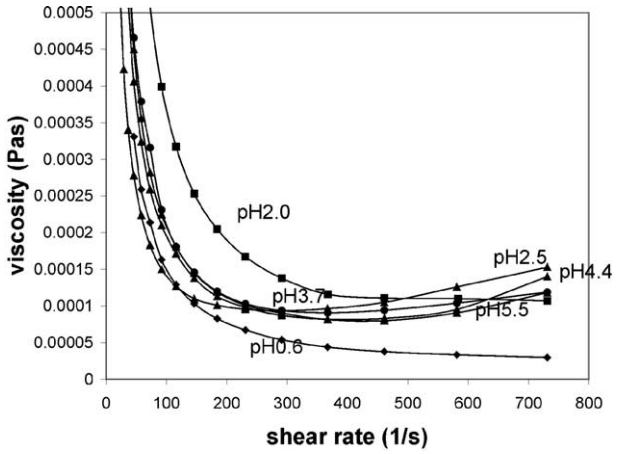

Fig. 11. The viscosity versus the shear-rate for EtOH suspensions containing 0.15 volume-fraction of $MoSi_2$ powder at different pH values.

3.5. Comparison of the surface species on Si_3N_4, SiC, $MoSi_2$ and SiO_2

It has been common wisdom that the surface species on Si_3N_4, SiC and $MoSi_2$ are Si–O-based. This investigation suggests the picture is more complex. The SiO_2 results are included in Fig. 1 for comparison . The surface of Si_3N_4 ($pH_{iep} = 9.0$), SiC ($pH_{iep} = 5.4$) and $MoSi_2$ ($pH_{iep} = 2.2$) must be oxide but not "SiO_2" as the pH_{iep} for SiO_2 is 1.4. From the XPS results (Table 1), the atomic % of O(1s) on the three powders ($Si_3N_4 = 13.14\%$, SiC = 13.71% and $MoSi_2 = 57.26\%$) are also different from SiO_2 (62.36%). Higher atomic% O(1s) (more oxide on the surface) corresponds to a lower pH_{iep} value. Si_3N_4 and SiC must be partially oxidized as they exhibit higher pH_{iep} values. The pH_{iep} difference between Si_3N_4 and SiC is due to surface amine groups on the Si_3N_4. $MoSi_2$ powder is completely covered by oxide but, because Mo species are included as Mo-oxide, the atomic% O(1s) is lower than for SiO_2. Thus $MoSi_2$ has a higher pH_{iep} value than SiO_2.

SiO_2 in EtOH (or H_2O) does not follow DLVO theory as the SiO_2 surface is covered by a gel-layer.[6,18,19] Si_3N_4/SiC/ and $MoSi_2$/EtOH on the other hand, follow DLVO theory and are demonstrated to do so via electrokinetic and rheological measurements.

4. Conclusions

Some of the surface species on Si_3N_4, SiC and $MoSi_2$ in EtOH are Si–O-based, however Si_3N_4 also has amine, SiC oxycarbides, and $MoSi_2$ Mo-oxide. Thus it was found the powder/suspension stabilities in EtOH are different from that of SiO_2 in EtOH. Ethanol is chosen as the EPD media as it always contains 0.2 wt.% H_2O which provides ions for electrostatic repulsion but is too spare to induce disruptive electrolysis. The assumption that the surface species on Si_3N_4, SiC and $MoSi_2$ in suspension is "Si–O" is thus too simplistic.

When Si-containing non-oxide ceramic powders (Si_3N_4, SiC, $MoSi_2$) are dispersed in EtOH, a pH-dependent electrical charge is induced, the charging mechanism being adsorption or desorption of protons on the surface sites.

Electrophoretic mobility results identify the isoelectric points (pH_{iep}) as 9.0 (Si_3N_4/EtOH), 5.4 (SiC/EtOH), 2.2 ($MoSi_2$/EtOH) and 1.4 (SiO_2/EtOH).

DLVO theory and the pH–V_T results define the stability of Si_3N_4, SiC and $MoSi_2$ ranges (Si_3N_4; pH <7 or pH >12, SiC; pH <5 or pH >6, and $MoSi_2$; pH >5). These results suggest colloidal stabilization is achieved by controlling the pH of the EtOH suspensions.

The stability-ratio was used to evaluate colloidal stability and indicates the same colloidal stability ranges. The viscosity and flow curves for the Si_3N_4/, SiC/ and $MoSi_2$/EtOH suspensions are pH dependent and, except for $MoSi_2$/EtOH, follow the Casson model over 0–300 s^{-1} shear-rates. The Casson yield stress values corresponded to the electrokinetic isoelectric points. The pH_{iep} values deduced from the flow curves agreed with those of electrokinetic measurements. $MoSi_2$/EtOH exhibited dilatancy and does not follow the Casson model.

References

1. Sarkar, P. and Nicholson, P. S., Electrophoretic deposition (EPD): mechanisms, kinetics, and application to ceramics. *J. Am. Ceram. Soc.*, 1996, **79**(8), 1987–2002.
2. Zhang, Z., Electrophoretic deposition forming of SiC-TZP composites in a nonaqueous sol media. *J. Am. Ceram. Soc.*, 1994, **77**(7), 1946–1949.
3. Mizuguchi, J., Sumi, K. and Muchi, T., A highly stable nonaqueous suspension for the electrophoretic deposition of powder substances. *J. Electrochem. Soc.*, 1983, **130**(9), 1819–1825.
4. Bouyer, F. and Foissy, A., Electrophoretic deposition of silicon carbide. *J. Am. Ceram. Soc.*, 1999, **82**(8), 2001–2010.
5. Wang, G., Sarkar, P. and Nicholson, P. S., Influence of acidity on the electrostatic stability of alumina suspensions in ethanol. *J. Am. Ceram. Soc.*, 1997, **80**(4), 965–972.
6. Wang, G., *Inonic Stability of Oxide Particles in Polar Organic Media*, Thesis, McMaster University, Ontario, Canada, 1998.
7. O'Brien, R. W. and White, L. R., Electrophoretic mobility of a spherical colloidal particle. *J. Chem. Soc. Faraday Trans.*, 1978, **2**(74), 1607.
8. Wang, G. and Nicholson, P. S., Heterocoagulation in ionically stabilized mixed-oxide colloidal dispersions in ethanol. *J. Am. Ceram. Soc.*, 2001, **84**, 6 1250-1256.
9. Bates, R. G., Paabo, M. and Robinson, R. A., Interpretation of pH measurements in alcohol–water solvents. *J. Phys. Chem.*, 1963, **67**, 1833.
10. Bergström, L. and Bostedt, E., Surface chemistry of silicon nitride powders: electrokinetic behaviour and ESCA studies. *Colloids and Surfaces*, 1990, **49**, 183–197.
11. Merle-Méjean, T., Abdelmounîm, E. and Quintard, P., Oxide layer on silicon carbide powder: a FT-IR investigation. *J. Molecular Structure*, 1995, **349**, 105–108.
12. Kitahara, A. and Furusawa, K., *Saishin Colloid Kagaku*. Koudansya, Japan, 1993.

13. Bleier, A., Fundamentals of preparing suspensions of silicon and related ceramic powders. *J. Am. Ceram. Soc.*, 1983, **66**, C–79-81.
14. Ged, Ph., Madar, R. and Senateur, J. P., Dielectric function of monocrystalline $MoSi_2$ by spectroscopic ellipsometry. *Phys. Rev. B*, 1984, **29**(12), 6981–6984.
15. Gregory, J., The calculation of Hamaker constants. *Adv. Colloid Interface Sci.*, 1969, **2**, 396–417.
16. Israelachvili, J. N., *Intermolecular and Surface Forces*. Academic Press, New York, 1985.
17. Casson, N., *A Flow Equation for Pigment-oil Suspensions of the Printing Ink Type, Rheology of Disperse Systems*. Pergamon Press, 1959.
18. Ketelson, H. A., Pelton, R. and Brook, M. A., Colloidal stability of stöber silica in aceton–water mixtures. *J. Colloid Interface Sci.*, 1996, **179**, 600.
19. Vigil, G., Zhenghe, X., Steinberg, S. and Israelachvili, J., Interactions of silica surfaces. *J. Colloid Interface Sci.*, 1994, **165**, 367.